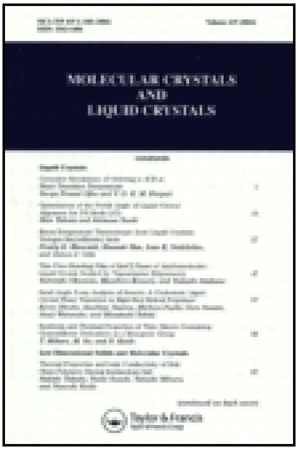

Molecular Crystals and Liquid Crystals
Publication details, including instructions for authors and subscription information:
http://www.tandfonline.com/loi/gmcl20

Influence of the Alkyl Spacer Length on the Phase Transition Behaviour of the λ-Shaped Liquid Crystal

Akihisa Yamaguchi [a] , Atsushi Yoshizawa [a] , Isa Nishiyama [b] , Jun Yamamoto [b] & Hiroshi Yokoyama [b]

[a] Department of Material Science and Technology, Faculty of Science and Technology, Hirosaki University, Hirosaki, Japan

[b] Yokoyama Nano-structured Liquid Crystal Project, ERATO, JST, Tokodai, Tsukuba, Japan

Version of record first published: 31 Aug 2006

To cite this article: Akihisa Yamaguchi, Atsushi Yoshizawa, Isa Nishiyama, Jun Yamamoto & Hiroshi Yokoyama (2005): Influence of the Alkyl Spacer Length on the Phase Transition Behaviour of the λ-Shaped Liquid Crystal, Molecular Crystals and Liquid Crystals, 439:1, 85/[1951]-95/[1961]

To link to this article: http://dx.doi.org/10.1080/15421400590956225

Mol. Cryst. Liq. Cryst., Vol. 439, pp. 85/[1951]–95/[1961], 2005
Copyright © Taylor & Francis Inc.
ISSN: 1542-1406 print/1563-5287 online
DOI: 10.1080/15421400590956225

Influence of the Alkyl Spacer Length on the Phase Transition Behaviour of the λ-Shaped Liquid Crystal

Akihisa Yamaguchi
Atsushi Yoshizawa
Department of Material Science and Technology, Faculty of Science and Technology, Hirosaki University, Hirosaki, Japan

Isa Nishiyama
Jun Yamamoto
Hiroshi Yokoyama
Yokoyama Nano-structured Liquid Crystal Project, ERATO, JST, Tokodai, Tsukuba, Japan

We reported that a novel λ-shaped liquid-crystalline molecule ***I-6*** *in which a cyanobiphenyl and two phenylpyrimidine groups are connected to 3, 4-dihydroxybenzoic acid exhibits an incommensurate SmA phase. In the present study, we have prepared the homologous series of the λ-shaped molecules* ***I-n*** *(****n*** *=* ***4****,* ***5****,* ***7****,* ***8****,* ***9****,* ***12****) and investigated effect of the spacer length on the phase transition behaviour. Compounds* ***I-4****,* ***I-8*** *and* ***I-12*** *with an even member of atoms in spacer showed the phase sequences of N-SmA-Cr or SmA-Cr. On the other hand, the odd members* ***I-7*** *and* ***I-9*** *showed the phase sequence of N-SmA-SmCanti-Cr.*

Keywords: liquid crystal; phase transition; smectic A, smectic Canti

1. INTRODUCTION

The driving force of mesophase formation is a fundamental topic in the investigation of molecular assembly systems. Recently, molecular topology [1] and microsegregation [2] have attracted much attention as

---

We thank Dr. Lianhui Qi of Yokoyama Nano-structured Liquid Crystal Project for XRD measurements. This work was partly supported by Aomori Prefecture Collaboration of Regional Entities for the Advancement of Technological Excellence, JST.

Address correspondence to Atsushi Yoshizawa, Department of Material Science and Technology, Faculty of Science and Technology, Hirosaki University, 3, Bunkyo-cho, Hirosaki 036-8561, Japan. E-mail: ayoshiza@cc.hirosaki-u.ac.jp

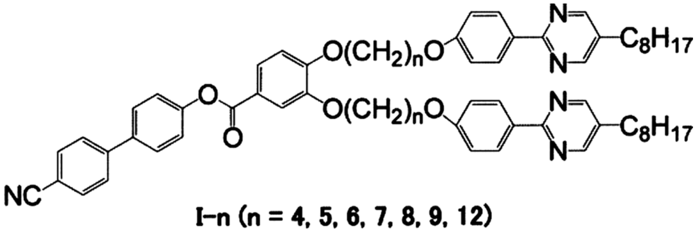

FIGURE 1 Molecular structure of the λ-shaped liquid-crystalline molecules **I-n**.

the origins for producing novel self-organizing systems. In addition, molecular motion is also important to understand the microscopic behaviour of liquid-crystalline molecules. Our C-13 NMR study of smectic liquid crystals revealed that (1) cooperative motion for the core parts contributes to the orientational order of the molecules in each layer and (2) inter-layer permeation of tails causes correlation between cores in adjacent layers [3]. Coupling or competition between intra-layer core-core interaction and inter-layer interaction can produce a new class of molecular aggregation. Recently we reported a novel λ-shaped liquid-crystalline molecule, 4-cyanobiphenyl-4′-yl 3, 4-bis{6-[4-(5-octylpyrimidin-2-yl)phenyloxy]hexyloxy} benzoate (**I-6**), as shown in Figure 1 [4]. The λ-shaped molecule **I-6** was found to realize a stable incommensurate SmA phase. Modification of the λ-shaped structure is expected to produce various organization of molecules. In the present study, we have prepared the homologous series of the λ-shaped molecules **I-n** (**n** = **4**, **5**, **7**, **8**, **9**, **12**) and investigated effect of the spacer length on the phase transition behaviour.

2. EXPERIMENTAL

Characterization of Materials

The purification of final products was carried out using column chromatography over silica gel (63-210 μm) (KANTO CHEMICAL Co., INC.) using a toluene-ethyl acetate mixture or a dichloromethane-ethyl acetate mixture as the eluent, followed by the recrystallization from an ethanol-chloroform mixture. The purity was checked by thin layer chromatography (TLC, aluminum sheets, silica gel 60 F254 from Merck). Dichloromethane was used as the solvent. Detection of products was achieved by UV irradiation (λ = 254 and 365 nm).

The structures of the final products were elucidated by infrared (IR) spectroscopy (BIO RAD FTS-30) and proton nuclear magnetic resonance (^{1}H NMR) spectroscopy (JEOL JNM-GX270). The analyses of the structures of the products by spectroscopic methods were found to be consistent with the predicted structures.

Liquid-Crystalline and Physical Properties

The initial phase assignments and corresponding transition temperatures for the final products were determined by optical polarized light microscopy using a Nikon Optiphot-pol polarizing microscope equipped with a Mettler FP82 hot stage and FP80 control processor. The heating and cooling rates were 5°C min^{-1}. The photomicrographs were taken using a camera (OLYMPUS DIGITAL CAMERA C-5050 ZOOM) in conjunction with a Nikon Optiphot-pol polarizing microscope. Temperatures and enthalpies of transition were investigated by differential scanning calorimetry (DSC) using a Seiko Instruments Inc. DSC6200. The materials were studied at a scanning rate of 5°C min^{-1} after being encapsulated in aluminum pans. The X-ray scattering experiments were performed using a real-time X-ray diffractometer (Bruker AXS D8 Discover). The monochromatic X-ray beam (Cu-Kα line) was generated by a 1.6 kW X-ray tube and Göbel mirror optics. The 2D position sensitive detector has 1024 × 1024 pixels in a 5 cm × 5 cm beryllium window. A sample was introduced into a thin glass capillary tube (diameter 1.0 mm), which was placed in a custom-made temperature stabilized holder (stability within ±0.1°C). The X-ray diffraction measurements and the textural observations by polarized light microscopy using a CCD camera were performed simultaneously on the sample in the glass capillary tube.

Preparation of Materials

4′-Cyanobiphenyl-4-yl 3,4-bis{4-[4-(5-octylpyrimidin-2-yl)phenoxy]butyloxy} benzoate (I-4)

5-Octyl-2-(4-hydroxyphenyl)pyrimidine (0.57 g, 2.0 mmol) purchased from Midori Kagaku Co., Ltd. and 1, 4-dibromobutane (0.86 g, 4.0 mmol) were dissolved in cyclohexanone (10 mL). Potassium carbonate (2.8 g, 2.0 mmol) was then added and the resulting mixture was stirred at 80°C for 6 h. The reaction mixture was filtered and the solvent was removed by evaporation under reduced pressure. The product was purified by column chromatography using dichloromethane as the eluent. 2-[4-(4-Bromobutyloxy)phenyl]-5-octylpyrimidine was obtained. Yield: 0.62 g (74%).

2-[4-(4-Bromobutyloxy)phenyl]-5-octylpyrimidine (0.62 g, 1.5 mmol) and ethyl 3, 4-dihydroxybenzoate (0.14 g, 0.74 mmol) were dissolved in cyclohexanone (10 mL). K_2CO_3 (0.20 g, 1.5 mmol) and KI (0.025 g, 0.15 mmol) were then added and the resulting mixture was stirred at 145°C for 12 h. The reaction mixture was filtered and the solvent was removed by evaporation under reduced pressure. The product was purified by column chromatography using a dichloromethane-ethyl acetate (20:1) mixture as the eluent, and recrystallized from an ethanol-chloroform (6:1) mixture (7 mL). Ethyl 3, 4-bis{6-[4-(5-octylpyrimidin-2-yl)phenyloxy]butyloxy}benzoate was obtained. Yield: 0.46 g (72%)

Ethyl 3, 4-bis{6-[4-(5-octylpyrimidin-2-yl)phenyloxy]butyloxy} benzoate (0.43 g, 0.50 mmol) was added to a solution of KOH (0.084 g, 1.5 mmol) in ethanol (95%, 10 mL). The resulting mixture was stirred under reflux for 2 h. The solution was acidified with HCl (concentrated, 1.0 ml). Water (15 mL) was added to the mixture and the aqueous phase was extracted with dichloromethane (3×20 mL). The organic extracts were combined, dried over Na_2SO_4, filtered and evaporated. 3, 4-Bis{6-[4-(5-octylpyrimidin-2-yl)phenyloxy]butyloxy} benzoic acid was obtained. Yield: 0.38 g (92%).

To a solution of 3, 4-bis{6-[4-(5-octylpyrimidin-2-yl)phenyloxy] butyloxy}benzoic acid (0.17 g, 0.20 mmol) in dichloromethane (10 mL), 4-cyano-4′-hydroxybiphenyl (0.040 g, 0.20 mmol), dicyclohexylcarbodiimide (0.042 g, 0.20 mmol) and 4-(N,N-dimethylamino) pyridine (0.003 g, 0.020 mmol) were added. The resulting solution was stirred at room temperature overnight. Precipitated materials were removed by filtration. After removal of the solvent by evaporation, the residue was purified by column chromatography on silica gel using a toluene-ethyl acetate (15 : 1) mixture. Recrystallization from ethanol gave the desired product. Yield: 0.14 g (67%).

δ_H (270 MHz, $CDCl_3$, TMS): 8.56 (d, 4H, Ar-H, J = 1.4 Hz), 8.34 (dd, 4H, Ar-H, J = 8.9 Hz, 3.0 Hz), 7.83 (dd, 1H, Ar-H, J = 8.5 Hz, 2.2 Hz), 7.74–7.60 (m, 7H, Ar-H), 7.33 (d, 2H, Ar-H, J = 8.9 Hz), 6.99–6.94 (m, 5H, Ar-H), 4.11 (t, 2H, $-OCH_2-$, J = 6.5 Hz), 4.10 (t, 2H, $-OCH_2-$, J = 6.5 Hz), 4.03 (t, 2H, $-OCH_2-$, J = 6.5 Hz), 4.02 (t, 2H, $-OCH_2-$, J = 6.5 Hz), 2.58 (t, 4H, $Ar-CH_2-$, J = 7.7 Hz), 1.90–1.27 (m, 32H, aliphatic-H), 0.88 (t, 6H, $-CH_3$, J = 6.6 Hz). ν/cm^{-1}(KBr): 2927, 2853 (C−H str.), 2224 (C≡N str.), 1728 (C=O str. −COO−), 1606, 1584 (C=C str.).

The other compounds presented in this paper were obtained by a similar method to that for **I-4**. Analytical data for the other compounds are given.

4′-cyanobiphenyl-4-yl 3,4-Bis{5-[4-(5-octylpyrimidin-2-yl) phenoxy]pentyloxy} benzoate (I-5)

δ_H (270 MHz, $CDCl_3$, TMS): 8.57 (d, 4H, Ar-H, J = 1.4 Hz), 8.37 (dd, 4H, Ar-H, J = 9.2 Hz, 3.0 Hz), 7.83 (dd, 1H, Ar-H, J = 8.5 Hz, 1.9 Hz), 7.74–7.60 (m, 7H, Ar-H), 7.32 (d, 2H, Ar-H, J = 8.4 Hz), 6.98–6.94 (m, 5H, Ar-H), 4.14 (t, 2H, $-OCH_2-$, J = 6.5 Hz), 4.13 (t, 2H, $-OCH_2-$, J = 6.5 Hz), 4.05 (t, 2H, $-OCH_2-$, J = 6.5 Hz), 4.04 (t, 2H, $-OCH_2-$, J = 6.5 Hz), 2.59 (t, 4H, Ar-CH_2-, J = 7.7 Hz), 1.90–1.27 (m, 44H, aliphatic-H), 0.88 (t, 6H, $-CH_3$, J = 6.6 Hz). ν/cm^{-1}(KBr): 2926, 2852 (C−H str.), 2223 (C≡N str.), 1726 (C=O str. −COO−), 1606, 1583 (C=C str.).

4′-Cyanobiphenyl-4-yl 3,4-bis{7-[4-(5-octylpyrimidin-2-yl) phenoxy]heptyloxy} benzoate (I-7)

δ_H (270 MHz, $CDCl_3$, TMS): 8.56 (s, 4H, Ar-H), 8.37 (dd, 4H, Ar-H, J = 9.2 Hz, 2.7 Hz), 7.83 (dd, 1H, Ar-H, J = 8.5 Hz, 1.9 Hz), 7.74–7.60 (m, 7H, Ar-H), 7.32 (d, 2H, Ar-H, J = 8.6 Hz), 6.99–6.93 (m, 5H, Ar-H), 4.10 (t, 2H, $-OCH_2-$, J = 6.5 Hz), 4.09 (t, 2H, $-OCH_2-$, J = 6.5 Hz), 4.02 (t, 2H, $-OCH_2-$, J = 6.5 Hz), 4.01 (t, 2H, $-OCH_2-$, J = 6.5 Hz), 2.59 (t, 4H, Ar$-CH_2-$, J = 7.7 Hz), 1.90–1,27 (m, 44H, aliphatic-H), 0.88 (t, 6H, $-CH_3$, J = 6.6 Hz). ν/cm^{-1}(KBr): 2927, 2853 (C−H str.), 2228 (C≡N str.), 1729 (C=O str. −COO−), 1607, 1583 (C=C str.).

4′-Cyanobiphenyl-4-yl 3,4-bis{8-[4-(5-octylpyrimidin-2-yl) phenoxy]octyloxy} benzoate (I-8)

δ_H (270 MHz, $CDCl_3$, TMS): 8.59 (s, 4H, Ar-H), 8.37 (d, 4H, Ar-H, J = 8.4 Hz), 7.83 (dd, 1H, Ar-H, J = 8.5 Hz, 2.2 Hz), 7.74–7.60 (m, 7H, Ar-H), 7.32 (d, 2H, Ar-H, J = 8.6 Hz), 6.99–6.92 (m, 5H, Ar-H), 4.09 (t, 2H, $-OCH_2-$, J = 6.5 Hz), 4.07 (t, 2H, $-OCH_2-$, J = 6.5 Hz), 4.02 (t, 2H, $-OCH_2-$, J = 6.5 Hz), 4.01 (t, 2H, $-OCH_2-$, J = 6.5 Hz), 2.60 (t, 4H, Ar$-CH_2-$, J = 7.7 Hz), 1.90–1,27 (m, 48H, aliphatic-H), 0.88 (t, 6H, $-CH_3$, J = 6.6 Hz). ν/cm^{-1}(KBr): 2925, 2853 (C−H str.), 2225 (C≡N str.), 1728 (C=O str. −COO−), 1606, 1584 (C=C str.).

4′-Cyanobiphenyl-4-yl 3,4-bis{9-[4-(5-octylpyrimidin-2-yl) phenoxy]nonyloxy} benzoate (I-9)

δ_H (270 MHz, $CDCl_3$, TMS): 8.56 (s, 4H, Ar-H), 8.37 (dd, 4H, Ar-H, J = 9.2 Hz, 2.7 Hz), 7.83 (dd, 1H, Ar-H, J = 8.5 Hz, 1.9 Hz), 7.74–7.60 (m, 7H, Ar-H), 7.32 (d, 2H, Ar-H, J = 8.6 Hz), 6.99–6.93 (m, 5H, Ar-H), 4.10 (t, 2H, $-OCH_2-$, J = 6.5 Hz), 4.09 (t, 2H, $-OCH_2-$, J = 6.5 Hz), 4.02 (t, 2H, $-OCH_2-$, J = 6.5 Hz), 4.01 (t, 2H, $-OCH_2-$, J = 6.5 Hz), 2.59 (t, 4H, $Ar-CH_2-$, J = 7.7 Hz), 1.90–1.27 (m, 52H, aliphatic-H), 0.88 (t, 6H, $-CH_3$, J = 6.6 Hz). ν/cm^{-1}(KBr): 2927, 2853 (C–H str.), 2228 (C≡N str.), 1729 (C=O str. –COO–),1607, 1583 (C=C str.).

4′-Cyanobiphenyl-4-yl 3,4-bis{12-[4-(5-octylpyrimidin-2-yl) phenoxy]dodecyloxy} benzoate (I-12)

δ_H (270 MHz, $CDCl_3$, TMS): 8.59 (s, 4H, Ar-H), 8.37 (d, 4H, Ar-H, J = 8.4 Hz), 7.83 (dd, 1H, Ar-H, J = 8.5 Hz, 2.2 Hz), 7.74–7.60 (m, 7H, Ar-H), 7.32 (d, 2H, Ar-H, J = 8.6 Hz), 6.99–6.92 (m, 5H, Ar-H), 4.09 (t, 2H, $-OCH_2-$, J = 6.5 Hz), 4.07 (t, 2H, $-OCH_2-$, J = 6.5 Hz), 4.02 (t, 2H, $-OCH_2-$, J = 6.5 Hz), 4.01 (t, 2H, $-OCH_2-$, J = 6.5 Hz), 2.60 (t, 4H, $Ar-CH_2-$, J = 7.7 Hz), 1.90–1.27 (m, 64H, aliphatic-H), 0.88 (t, 6H, $-CH_3$, J = 6.6 Hz). ν/cm^{-1}(KBr): 2928, 2855 (C–H str.), 2223 (C≡N str.), 1727 (C=O str. –COO–), 1606, 1585 (C=C str.).

3. RESULTS AND DISCUSSION

Phase Transition Behaviour

Transition temperatures and transition enthalpies for the homologous series of λ-shaped liquid-crystalline molecules **I-n**, measured by optical polarized light microscopy and differential scanning calorimetry (DSC) are listed in Table 1. A large odd-even effect on the clearing temperatures is apparent in which the even members of the series exhibit the higher values. The enthalpy changes associated with the

TABLE 1 Transition Temperatures (°C) and Transition Enthalpies (kJ mol^{-1}) (in Square Brackets) for **I-n**

n	Phase transition temperatures
4	Iso 209[15.7] SmA 109[27.1] recryst. mp 133
5	Iso 148[1.9] N 144[0.95] SmA 100[45.2] recryst. mp 128
6	Iso 183[7.9] N 177[1.1] SmA 157[0.65] SmAinc 113[39.2] recryst. mp 150
7	Iso 145[2.4] N 129[4.2] SmA 127[3.0] SmCanti 64[25.2] recryst. mp 130
8	Iso 166[8.7] N 162[8.8] SmA 112[46.6] mp 148
9	Iso 141[4.4] N 137[7.6] SmA 132[0.95] SmCanti 56[21.7] recryst. mp 127
12	Iso 150[23.2] SmA 81[34.7] recryst. mp 118

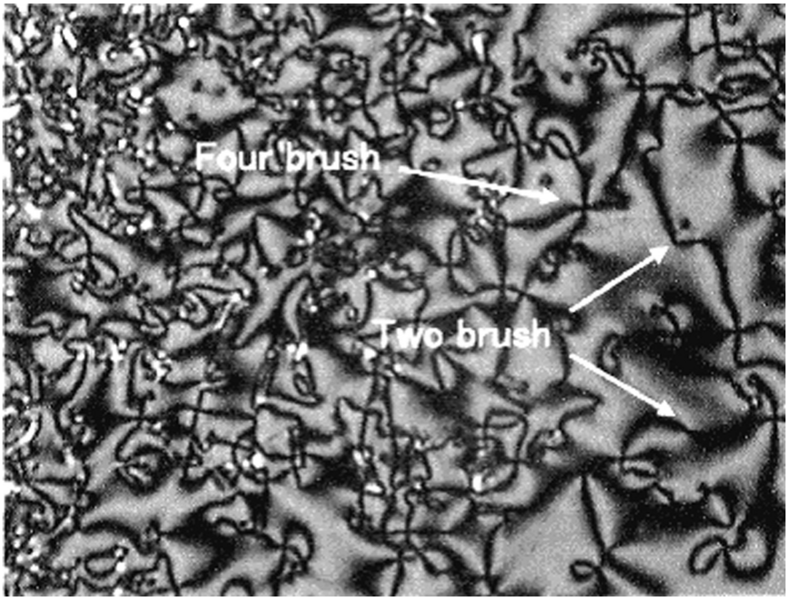

FIGURE 2 A photomicrograph of the SmCanti phase in a pseudo-homeotropically aligned region for compound **I-7**.

Iso-N transition for the series also show a pronounced alternation as the length and parity of the spacer is varied. The values for the Iso-N enthalpy for the even members are several times larger than those for the odd members. All of the homologous series studied here showed the SmA phase. As our previous report, **I-6** exhibited an unusual incommensurate SmA (SmAinc) phase [4]. In this study, the homologous series except for **I-6** did not show the SmAinc phase. It is noted that some of the odd members, **I-7** and **I-9**, showed the SmCanti phase. The marked odd-even effect on the phase sequence is apparent. A photomicrograph of the SmCanti phase in a pseudo-homeotropically aligned region for **I-7** is shown in Figure 2. The *Schlieren* textures clearly showed two and four brush singularities of the smectic phase. The two brush singularities are not allowed to be formed in the synclinic phase but can be generated with anticlinic ordering [5].

X-ray Diffraction Studies

Figure 3 shows intensity profiles of the wide angle X-ray scattering for the homologous series of the λ-shaped compounds **I-n**. Diffuse scattering in the wide angle region was observed for all of the smectic phases

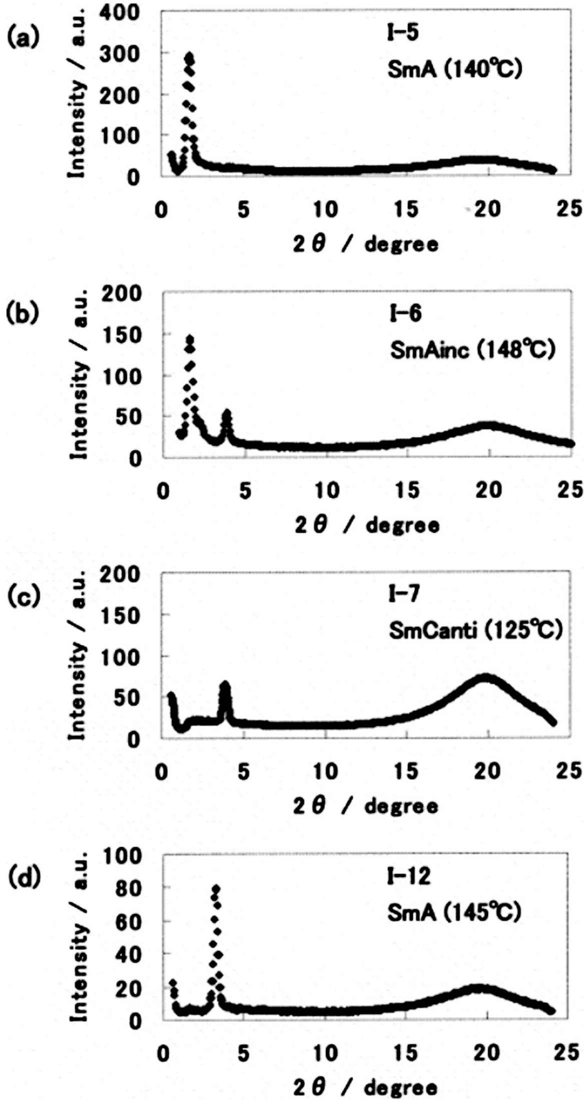

FIGURE 3 X-ray scattering patterns of **I-n**.

of the homologues, indicating that there is no long range positional order within the layers. The estimated molecular length (l) from MM2 calculation and the layer spacing (d) obtained from the X-ray scattering experiments are summarized in Table 2. The obtained layer spacings of the SmA phase for **I-5** and **I-6** were about 52 and 55 Å

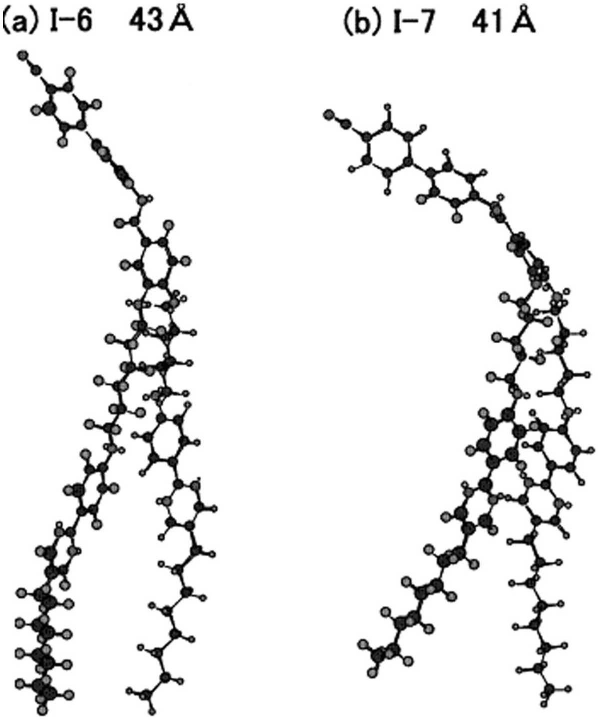

FIGURE 4 Expected molecular configurations and lengths by the MM2 method.

whereas the estimated molecular lengths were about 38 and 43 Å respectively. The longer layer spacings than the molecular lengths suggest the formation of an interdigitated layer structure for the SmA phases of **I-5** and **I-6**. On the other hand, the obtained layer spacings of the SmCanti phase for **I-7** and the SmA phase for **I-12**

TABLE 2 Molecular Lengths (l) and Layer Spacings (d) of **I-n**.

Compound	Mesophase	l/Å[a]	d/Å[b]
I-5	SmA	38	52
I-6	SmA	43	55
	SmAinc		55, 40, 23
I-7	SmCanti	41	22.7
I-12	SmA	50	27.2

[a] Estimated by MM2 calculation.

[b] Calculated from the X-ray diffraction peak that appeared in the small angle region.

were about 23 and 27 Å whereas the molecular lengths were estimated to be about 41 and 50 Å respectively. The approximately half layer spacings compared to the molecular lengths suggest the smectic phases form an intercalated layer structure [6]. The ability to accommodate the terminal chains in the space between the intercalated layers of mesogenic groups is determined largely by the length of the spacer. Thus, for the intercalated phases to be observed the terminal chain must be equal to or shorter in length than the spacer. If the terminal chain is considerably longer than the spacer, then interdigitated phases are observed [6]. For compound **I-6** in which the terminal chain is equal to the spacer, thus the intermediate state appeared. Three periodic density waves were observed in the SmAinc phase, indicating that interdigitated, intercalated and monolayered structures coexist [4].

Then we discuss the appearance of the SmCanti phase for the odd members. Estimated molecular lengths and configurations calculated by the MM2 method for **I-6** and **I-7** are also shown in Figure 5. The odd member **I-7** was found to adopt more bent configuration compared to the even member **I-6**. The bent configuration seems to be reasonable for the formation of the intercalated SmCanti phase for **I-7**. However, the odd member **I-5** with bent configuration showed no SmCanti phase. This is considered to be due to the difference of the layer structure between **I-5** and **I-7**, i.e., **I-5** has the interdigitated smectic phase whereas **I-7** has the intercalated one.

4. CONCLUSIONS

We have prepared the homologous series of the λ-shaped liquid-crystalline molecules and investigated the phase transition behaviour. XRD studies indicate that appearance of the SmAinc phase for **I-6** in which the terminal chain is equal to the spacer results from competition between interdigitated and intercalated layer structures. A marked odd-even effect on transition behaviour was observed. It is noted that some of the odd members, **I-7** and **I-9**, showed the SmCanti phase.

REFERENCES

[1] Goodby, J. W., Mehls, G. H., Saez, I. M., Tuffin, R. P., Mackenzie, G., Auzély-Velty, R., Benvegnu, T., & Plusquellec, D. (1998). *Chem. Commun.*, 2057.

[2] (a) Tschierske, C. (2000). *J. Mater. Chem.*, *11*, 2647.
(b) Tschierske, C. (1998). *J. Mater. Chem.*, *8*, 1485.

[3] Yoshizawa, A., Kikuzaki, H., & Fukumasa, M. (1995). *Liq. Cryst.*, *18*, 351.

[4] Yamaguchi, A., Nishiyama, I., Yamamoto, J., Yokoyama, H., & Yoshizawa, A. (2005). *J. Mater. Chem.*, *15*, 280.

[5] (a) Takanishi, Y., Takezoe, H., Fukuda, A., & Watanabe, J. (1992). *Phys. Rev. B*, *45*, 7684.
  (b) Takanishi, Y., Takezoe, H., Fukuda, A., Komura, H., & Watanabe, J. (1992). *J. Mater. Chem.*, *2*, 71.

[6] Imrie, C. T. & Luckhurst, G. R. (1998). In: *Handbook of Liquid Crystals Vol. 2B: Low Molecular Weight Liquid Crystals*, Demus, D., Gray, J. W., Spiess, H.-W., & Vill, V. (Eds.), Wiley-VCH: Weinheim, Chapter X, 801.